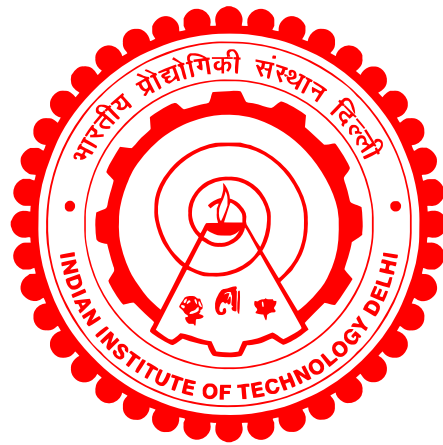


**MOLECULAR DYNAMICS STUDY OF
STRUCTURE FORMATIONS IN STRONGLY
COUPLED PLASMA**

Mamta



DEPARTMENT OF PHYSICS

INDIAN INSTITUTE OF TECHNOLOGY DELHI

September 2025

© Indian Institute of Technology Delhi (IITD), New Delhi, 2025

Molecular Dynamics Study of Structure Formations in Strongly Coupled Plasma

by

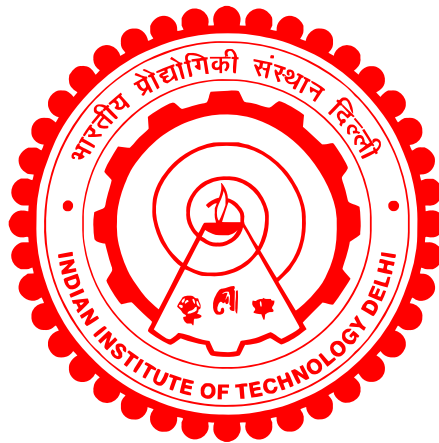
Mamta

Department of Physics

Submitted

in partial fulfillment of the requirements of the degree of Doctor of Philosophy

to the



INDIAN INSTITUTE OF TECHNOLOGY DELHI

September 2025

Dedicated to my family and friends

Certificate

This is to certify that the thesis entitled “**Molecular Dynamics Study of Structure Formations in Strongly Coupled Plasma** ”, submitted by **Mamta** to the Indian Institute of Technology Delhi, for the award of the degree of **Doctor of Philosophy** in PHYSICS, is a record of the original, bona fide research work carried out by her under my supervision and guidance. The thesis has reached the standards fulfilling the requirements of the regulations related to the award of the degree.

The results contained in this thesis have not been submitted in part or in full to any other University or Institute for the award of any degree or diploma to the best of my knowledge.

Prof. Amita Das

Department of Physics,
Indian Institute of Technology Delhi.

Date:

Acknowledgements

I would like to take this opportunity to extend my deep gratitude to my dedicated supervisor, Prof. Amita Das, for her unwavering guidance throughout my research. I consider myself privileged to have the chance to work under her direction. I am sincerely appreciative of her kindness, and encouragement, and for consistently inspiring me to engage in critical thinking and pursue excellence. She has consistently been accessible to listen to me and engage in talks about my research work with great patience. Throughout the difficult period of the COVID-19 pandemic, she remained always approachable. Her profound understanding of research issues, methodology for addressing these challenges, ability to elegantly link disparate problems, and exceptional writing skills have regularly inspired me. Completing this thesis would have been impossible without her exceptional help and encouragement. I will always recall one of her statements: "Life is extremely challenging; we must strive for positive outcomes." Through her guidance, I acquired the abilities to be a skilled researcher and a commendable person.

I also want to express my gratitude to my SRC members Prof. G. Vijaya Prakash, Prof. Ramesh Narayanan, and Prof. Vikrant Saxena for their careful oversight of my progress throughout the Ph.D. program. Their helpful suggestions have constantly inspired me to do better in my work.

I want to thank my collaborators, Dr. Srimanta Maity, Ms. Priya Deshwal, Mr. Aman Singh Katariya, and Dr. Animesh Sharma for the extensive conversations that helped me to resolve significant physics challenges in my research work.

I address sincere thanks to all members of the Einstein Research Scholar Room for maintaining a peaceful and inviting environment in the laboratory. My special thanks to Mr. Subhasish Bag and Mr. Aman Singh Katariya for their insightful discussions on numerous topics that enhanced my understanding of my research area. I would like to express heartfelt thanks to Mr. Trishul Dhalia, Mr. Subramanya Bhat, Mr. Imran Khan, and Mr. Rohit Juneja for their unwavering support and emotional assistance throughout my moments of vulnerability. Every time I am in need of help of any kind, they are there for me and support me in every circumstance. I have not only gained excellent labmates but also friends to cherish for a lifetime. Additionally, I would like to extend my warmest regards to my junior, Mr. Yasir, for providing a friendly environment.

I like to show my greatest gratitude to my closest friend, Ms. Priya Deshwal, who has remained rigidly by my side throughout every phase of my journey. Her constant support, encouragement, and compassionate behavior have constituted my paramount strength. Beyond friendship, she has shared a sisterly bond, participating in my victories with equal empathy and happiness.

My research would not have been possible without the financial aid provided by the University Grants Commission (UGC), to which I would like to express my gratitude. I appreciate the financial assistance afforded by the travel grant (Research Scholar Travel Award (RSTA)) from IIT Delhi, which financed my attendance at conferences.

Finally, I wish to convey my profound gratitude to my family for their constant encouragement throughout this extensive journey. I extend my profound thanks to my parents, Mrs. Mukesh Devi and Mr. Sukhbir Singh, and my siblings, Mr. Hitesh Yadav, Ms. Reena and Mrs. Vandana for their patience, unwavering efforts, and the faith they have shown in me. Their influence on my success is incalculable and never be repaid.

No one has endured this experience as profoundly as my life partner, Mr. Arjun Yadav. I am eternally grateful for his patience and solace. You support me in all my situations, and together we share some of my most cherished moments. The care, and love he has lavished are irreplaceable and have been the strength to keep going. I eagerly anticipate the journey ahead, confident it will be exciting and filled with adventure. Thank you for encouraging my thoughts, emotions, and essence. I am genuinely fortunate to have him as a continual presence in my life. I would like to convey sincere thanks to my mother and father-in-law, Mrs. Sarita Singh and Mr. Surender Singh Yadav, for their kindness and support throughout this journey. Also, I want to add special thanks to my brother-in-law, Mr. Vikram Singh Yadav, for always supporting me through my ups and downs and for being a steadfast source of emotional assistance. Above all, I thank my little angel, Taksh. Before I ever touched his tiny hands, he touched my soul—becoming my greatest source of strength, love, and inspiration. This thesis, and every step that led to it, carries the rhythm of his unseen companionship. You are the most beautiful chapter of my life, and this work is as much yours as it is mine.

Mamta

Abstract

This thesis focuses on the study of structure formations and their dynamics in strongly coupled plasma regimes with the help of Molecular Dynamics (MD) simulations using an open-source code LAMMPS (Large-scale Atomic/Molecular Massively Parallel Simulator).

The work primarily concentrates on the two strongly coupled regimes of plasma physics i.e. Ultracold plasma and Dusty plasma. In ultracold plasma, the study examines the formation of classical bound structures and also understands the shielding profile in a strongly coupled regime. At equilibrium, various kinds of classical bound structures have been observed. Another aspect of this regime, i.e., the shielding profile, is understood by externally inserting a highly charged particle, which mimics a probe in experiments. The crystalline structures have been observed around this externally inserted particle in two- and three-dimensional simulations. The potential profile of the shielding cloud has been compared with the Debye shielding profile. Also, the dynamics of the shielding cloud have been observed under the influence of external forces.

In dusty plasma medium, the transition of the dynamics of dust clusters from the macroscopic to the microscopic regime passing through the mesoscopic regimes has been studied. These regimes are classified depending on the ratio of particles on the surface to the bulk in the dust cluster, similar to that observed in the condensed matter. The emergence of an extra ring with the addition of particles, is always preceded by structures exhibiting pentagonal symmetry in the core. The dependence of the formation of pentagonal structures under various symmetry of boundary conditions (square, hexagonal, and pentagonal) has been studied in detail.

सार

यह शोधप्रबंध दृढ़ युग्मित प्लाज़्मा में संरचना निर्माण तथा उनकी गतिकी के अध्ययन पर केंद्रित है। इस अध्ययन में आणविक गतिकी अनुकरण की सहायता ली गई है, जिसके लिए मुक्त स्रोत संहिता LAMMPS (विशाल-पैमाने परमाण्विक/आणविक बहुल-समन्वित अनुकरणकर्ता) का उपयोग किया गया है।

यह कार्य मुख्यतः प्लाज़्मा भौतिकी के दो दृढ़ युग्मित क्षेत्रों – अर्थात् अत्यंत शीतल प्लाज़्मा और धूलिकणीय प्लाज़्मा – पर केंद्रित है। अत्यंत शीतल प्लाज़्मा के अध्ययन में पारंपरिक बंधित संरचनाओं के निर्माण की जांच की गई है तथा दृढ़ युग्मित अवस्था में आवरण की रूपरेखा को समझने का प्रयास किया गया है। संतुलन की अवस्था में विभिन्न प्रकार की पारंपरिक बंधित संरचनाएँ देखी गई हैं। इस क्षेत्र का एक अन्य पहलू, अर्थात् आवरण की रूपरेखा, को समझने के लिए बाहरी रूप से एक अत्यधिक आवेशित कण डाला गया है, जो प्रयोगों में प्रयुक्त जांच कण की तरह कार्य करता है। इस बाहरी रूप से डाले गए कण के चारों ओर द्वि-आयामी तथा त्रि-आयामी अनुकरणों में स्फटिकीय संरचनाएँ देखी गई हैं। आवरण मेघ की विभव रूपरेखा की तुलना डेबाई आवरण की रूपरेखा से की गई है। साथ ही, बाहरी बलों के प्रभाव में आवरण मेघ की गतिकी का भी अवलोकन किया गया है।

धूलिकणीय प्लाज़्मा माध्यम में, धूलिकण समूहों की गतिकी का संक्रमण मध्यवर्ती स्तर से होते हुए स्थूल स्तर से सूक्ष्म स्तर की ओर परिवर्तन का अध्ययन किया गया है। इन स्तरों का वर्गीकरण धूलिकण समूह में सतह पर स्थित कणों और आंतरिक कणों के अनुपात पर निर्भर करता है, जो कि संघनित पदार्थ में देखे गए व्यवहार के समान है। पंचभुजीय सममिति वाली संरचनाएँ हमेशा केंद्र में प्रकट होती हैं जब भी कणों के जुड़ने के साथ एक अतिरिक्त वलय उत्पन्न होता है। सीमा स्थितियों (वर्गाकार, षट्भुजाकार, तथा पंचभुजाकार) की विभिन्न सममितियों के अंतर्गत पंचभुजीय संरचनाओं के निर्माण की निर्भरता का विस्तृत अध्ययन किया गया है।

Contents

Certificate	i
Acknowledgements	ii
Abstract	iv
सार	v
Contents	vi
List of Figures	ix
List of Tables	xv
1 Introduction	1
1.1 Background	3
1.1.1 Coulomb coupling parameter (Γ)	5
1.1.2 Ultracold neutral plasma	7
1.1.3 Dusty plasma	8
1.2 Methodology	10
1.3 Previous work and motivation	12
1.4 Thesis Organisation	15
2 Structure formation by electrostatic interactions in strongly coupled ultracold neutral plasma medium	20

2.1	Introduction	21
2.2	Simulation details	23
2.3	Formation of bound structures: At equilibrium	26
2.4	Structure formation in a perturbed system: 2D	32
2.4.1	The structure of shielding cloud	33
2.4.2	Impact on bound structures in bulk	37
2.5	External perturbation in three-dimensional (3D) system	37
2.5.1	Form of the shielding cloud	39
2.5.2	Time evolution of shielding cloud in 3D	41
2.5.3	Comparison with Debye shielding	42
2.6	3D bound structures	44
2.7	Conclusion	49
3	Evolution of shielding cloud under oscillatory external forcing in strongly coupled UNP	51
3.1	Introduction	52
3.2	Simulation Details	53
3.3	Behavior of shielding cloud in the presence of external oscillatory and spatially homogeneous forcing	54
3.3.1	Time series analysis	58
3.3.2	Parametric studies	60
3.4	Oscillatory charge as an external perturbation	63
3.5	Summary and conclusion	69
4	Bulk and surface dominated phenomena and the formation of pentagonal structures in 2-D strongly coupled finite dust clusters	71
4.1	Introduction	72
4.2	Description of MD simulation details	73
4.3	Equilibrium pattern formation	75
4.4	Pentagonal structures	81
4.4.1	Role of the symmetry of confining potential	83
4.4.2	Role of screening	86
4.5	Summary and conclusion	89
5	Summary, Conclusions and Future scope	91
5.1	Summary of the thesis	92
5.2	Future prospects	94
5.2.1	Dynamics and stability of bound structures under the influence of time-dependent external perturbation	95
5.2.2	Dynamics of shielding cloud in 3D under the influence of oscillatory external forcing	96
5.2.3	Study of extended and shaped dust particles	96

5.2.4	Formation of three-dimensional (3D) bound structures	97
5.2.5	Magnetized dust particles	98
5.2.6	Pattern formation and dynamics of dust grain clusters in ultra-cold regime	98
Bibliography		99
Appendix A Potential energies for bound structures having nine particles		122
A.1	Potential energies for bound structures	122
List of Publications		126
Bio-data		129

List of Figures

2.1	Pictorial representations of distinct variety of classical bound structures at equilibrium. The blue and red dots represent the ions and electrons, respectively. Here, the mass of ions is chosen to be $M_{ion} = 100m_e$	27
2.2	Pictorial representation of the transition of classical bound structure from a linear chain structure to square-shaped structure with the evolution of time. The blue and red dots represent the ions and electrons, respectively.	29
2.3	Schematic representation of classical bound structures at equilibrium when $M_{ion} = 1836m_e$. The blue and red dots represent the ions and electrons, respectively.	30
2.4	Pictorial representation of the time evolution of one kind of classical bound structure. At $t\omega_{pe} = 0$ the pictorial representation of the distribution of ions and electrons initially in the simulation box is shown. The evolution of bound structure is shown from $t\omega_{pe} = 0.2034$ to 0.45 . The blue and red dots correspond to ions and electrons, respectively.	31
2.5	Schematic representation of the evolution of the ring-shaped bound structure. The transition state between the (b) and (c) subplots is represented by the colored inset. Similarly, the transition state between (c) and (d) is also shown by the colored inset. The evolution of bound structure is shown from $t\omega_{pe} = 0.2034$ to 0.5 . The red and blue dots correspond to electrons and ions.	32
2.6	Arrangements of electrons (represented by red dots) around external perturbation (represented by green dots). The external perturbation is introduced at the center of the simulation box.	33
2.7	Radial distribution function (RDF) as a function of normalized distance from the external perturbation at time $t\omega_{pe} = 54.9$	34
2.8	Voronoi diagram of electrons (red dots) around the external perturbation. Voronoi cells in yellow color represent the six nearest neighbors, whereas cyan color shows five neighbors.	35

2.9	Potential profile as a function of normalized distance (r/λ_D) from the external perturbation. The solid blue curve corresponds to potential in normal electron-ion plasma (Debye shielding), and the dotted red curve is in ultracold neutral plasma (numerical shielding).	36
2.10	Pictorial representation of the evolution of shielding cloud around the external perturbation. The green, red, and blue dots correspond to externally introduced perturbation, electrons, and ions, respectively.	38
2.11	Schematic representation of complex bound structures formed in the bulk of plasma when the external perturbation is introduced.	39
2.12	The projection of all the electrons that are involved in shielding cloud around the external perturbation (green dot) in (a) horizontal plane ($x-y$) and (b) vertical plane ($x-z$)	40
2.13	Shell structure by the projection of all the electrons into the ($\rho-z$) plane. Most occupied shells are denoted by black dotted lines, and the green dot corresponds to the external perturbation.	41
2.14	Radial distribution function (RDF) as a function of normalized distance from the external perturbation at ($t\omega_{pe}=218.7$).	42
2.15	Voronoi diagram with two different orientations for electrons in the first shell [shown in subplot (a), (b)], second shell [shown in subplots (c), (d)] and in the third shell [shown in subplots(e, f)] having 12, 20, and 50 electrons, respectively.	43
2.16	Number of electrons (N) in the shielding cloud near the external perturbation. Inset (a) shows the zoomed plot of the highlighted portion.	44
2.17	Plot of potential profile as a function of normalized distance from external perturbation having charge $100Q_{ion}$ and value of LJ parameter (σ) is $8.64 \times 10^{-9}m$, i.e., smaller than the Debye length (λ_D) 7.88×10^{-8} m. Here, the blue and red curves correspond to the potential in normal electron-ion plasma and ultracold neutral plasma, respectively, and subplot (a) represents the zoomed plot of the rectangular region shown by dotted lines.	45
2.18	Plot of potential profile as a function of normalized distance from external perturbation. Here, the value of LJ parameter (σ) is 8.64×10^{-8} m, i.e., larger than the Debye length (λ_D) 7.88×10^{-8} m. Here, the blue and red curves correspond to the potential in normal electron-ion plasma and ultracold neutral plasma, respectively.	46
2.19	Schematic representation of initial and final states of bound structures in 3D (without background plasma). Here, red and blue dots correspond to electrons and ions, and subplots (a), (c), and (e) represent the initial states, whereas subplots (b), (d), and (f) show the final states.	47
2.20	Pictorial representation of the overlapping ringed and cuboid structures.	48

2.21	Plot of the total potential energy of the overlapping ringed (green) and cuboid structure (magenta) as a function of interparticle spacing which is normalized with the LJ parameter σ . Here, the star represents the minima in the potential energy and the zoomed view of the minima is shown in the inset.	49
3.1	The schematic representation for the arrangements of electrons in the shielding cloud around the external perturbation. The red, blue, and green colors represent the electrons, ions, and external perturbation, respectively.	54
3.2	Temporal evolution of four distinct particles selected from separate shells around the static charge particle over the time duration $t\omega_{pe} = 0.1689 - 0.4360$. The color variation from blue to red represents the time evolution of particles. Here, the amplitude (E_0) and frequency (ω_0) of the applied field are 100 V/m and $10\omega_{pe}$, respectively.	55
3.3	The time evolution of angular displacement for one of the particles from the cluster with changing the amplitude of the oscillatory electric field E_0 . The blue and red curves correspond to amplitudes of 100 V/m and 101 V/m, respectively. The magenta curve shows the variation of the oscillatory electric field ($E_0 \sin(\omega_0 t)$) with the normalized time ($t\omega_{pe}$).	56
3.4	The time evolution of angular displacement for one of the particles from the cluster. The amplitude and frequency of the oscillatory electric field are 100 V/m and $10\omega_{pe}$, respectively. This is the case when we simulate the system in the absence of background plasma.	58
3.5	Variation of average displacement (ds) with the radius for two different amplitudes 100 V/m (solid blue curve) and 101 V/m (dashed magenta curve) of the oscillatory electric field.	59
3.6	Time evolution of V_θ for one of the particles from the cluster for two different amplitudes of the oscillatory electric field. The blue solid curve and red dashed curve correspond to the amplitude 100 V/m and 101 V/m, respectively.	60
3.7	Variation of correlation dimension with the embedding dimension for two amplitudes of the uniform electric field. The blue and red curves correspond to the E_0 100 V/m and 101 V/m, respectively.	61
3.8	Particle trajectory of one particle from each shell over the time duration $t\omega_{pe} = 0.1794 - 0.5123$. The color variation from orange to red shows the time evolution of particles. The amplitude and frequency of the applied oscillatory uniform electric field are 500 V/m and $10\omega_{pe}$, respectively.	62
3.9	The time evolution of angular displacement for one of the particles from the cluster having an amplitude and frequency of the oscillatory uniform electric field is E_0 is 500 V/m and $10\omega_{pe}$. The inset represents the zoomed view of oscillations, which is shown by a colored box. The magenta curve shows the variation of the oscillatory uniform electric field ($E_0 \sin(\omega_0 t)$).	63

- 3.10 The time evolution of angular displacement for one of the particles from the cluster. The amplitude and frequency of the oscillatory uniform electric field are 100 V/m and $15\omega_{pe}$. The inset represents the zoomed view of oscillations, which is shown by a colored box. The magenta curve shows the variation of the oscillatory spatially uniform electric field ($E_0 \sin(\omega_0 t)$). 63
- 3.11 (a) Variation of correlation dimension with the amplitude (E_0) of oscillatory electric field for three different embedding dimensions. (b) Variation of correlation dimension with the frequency (ω_0) of the external applied oscillatory electric field. The circle, square, and diamond shapes correspond to four, five, and six embedding dimensions, respectively. 64
- 3.12 The time evolution of the angular displacement (θ) for one particle chosen randomly from the cluster. The amplitude and frequency of the oscillatory electric field are 100 V/m and $10\omega_{pe}$, respectively. Here, the temperature is chosen to be 0.01 K. 65
- 3.13 Schematic representation of the dynamics of the cluster over the time duration $t\omega_{pe} = 2$. The blue sinusoidal curve shows the time variation of $q_0 + q_1 \sin(\omega_0 t)$ (for $q_1 = 20$), and the yellow sphere on this curve represents the corresponding subplots. 66
- 3.14 Schematic representation of the dynamics of the cluster over the time duration $t\omega_{pe} = 2.6$. The blue sinusoidal curve shows the time variation of $q_0 + q_1 \sin(\omega_0 t)$ (for $q_1 = 50$) and the yellow sphere on this curve represents the corresponding subplots. 67
- 3.15 The variation of angle α (degree) values between two nearest neighbors (red dots) from a reference particle (green dot) along with normalized time. The inset shows how the value of α is calculated. The green and red dots represent the reference particle and the electrons near this reference particle, respectively. 68
- 4.1 Subplots (a), (d) represent the arrangements of particles initially for $N_T = 13$ and 100, respectively. Particle trajectory for $N_T = 13$ over the time duration (b) $t\omega_{pd} = 0 - 1000$ and (c) $t\omega_{pd} = 1000 - 2000$. These show the intershell dynamics of the particles. Whereas, particle trajectory for $N_T = 100$ over the time duration (e) $t\omega_{pd} = 0 - 1000$ and (f) $t\omega_{pd} = 1000 - 2000$. These show the rigid dynamics of the cluster. 76
- 4.2 Plot of ratio (number of particles on surface/number of particles in the bulk) to the total number of dust particles. Here, three different regions show the microscale, mesoscale, and macroscale. The mesoscale (represented by yellow shade) shows the transition regime between intershell dynamics and rigid dynamics. The microscale and macroscale correspond to intershell and rigid dynamics, respectively. 77
- 4.3 Trajectory of all the particles over time duration $t\omega_{pd} = 100$. Subplots (a) and (b) correspond to particles 33 and 37, respectively. Here, the color from blue to magenta shows the time evolution of particles. 78

4.4	Trajectory of all the particles over the duration $t\omega_{pd} = 100$. Subplots (a) and (b) correspond to $N_p = 41, 42$, respectively. Here, the color variation from blue to magenta represents the evolution of particles.	79
4.5	(a) Time evolution of average angular displacement ($\theta(t)$) for $N_p = 47$. (b) The Fourier transform of $\theta(t)$ as a function of normalized frequency ω . . .	80
4.6	(a) Particle trajectory for $N_p = 80$. Here, the color variation from magenta to yellow shows the evolution of time. (b) Time evolution of average angular displacement ($\theta(t)$) for $N_p = 80$	81
4.7	Formation of pentagon structure when a new shell is added. The magenta dots represent the position of particles, and the blue dotted lines show the formation of pentagon structures. The green-colored spherical markers show the value of N_T when structures with pentagonal symmetry get formed. The first pentagon appears in a single-ringed structure of (0,5). . .	82
4.8	Formation of pentagonal structures with the total number of particles in different confinement boundaries. The green-colored spherical markers represent the presence of pentagonal structures, and the yellow cross represents the missed pentagonal structures earlier obtained in radial confinements.	84
4.9	Trajectory of $N_p = 15$ in different confinements. Subplot (a) The trajectory of one particle from each shell in square confinement over the duration $t\omega_{pd} = 400$. Subplots (b) and (c) show the trajectory of all particles in the pentagon ($t\omega_{pd} = 400$) and hexagon ($t\omega_{pd} = 400$) shaped confinements. Here, color variation from blue to green shows the evolution of particles. In this case, the screening parameter ($\kappa = 1$)	86
4.10	Trajectory of $N_p = 15$ in different confinements. Subplot (a) The trajectory of one particle from the outer shell and all particles from the inner shell in square confinement over the duration $t\omega_{pd} = 3350$. Subplots (b) and (c) show the trajectory of all particles in the pentagon ($t\omega_{pd} = 500$) and hexagon ($t\omega_{pd} = 400$) shaped confinements. Here, color variation from blue to green shows the evolution of particles. In this case, the screening parameter (κ) is two.	87
5.1	The schematic representation of the evolution of one kind of bound structure having net charge is zero with the normalized time ($t\omega_{pe}$). The amplitude and frequency of the applied uniform oscillatory electric field are 10^5 V/m and $10\omega_{pe}$, respectively. Here, blue and red dots correspond to ions and electrons, respectively.	95
5.2	Diagrammatic representation of the bound structure having zero net charge, with normalized time ($t\omega_{pe}$). Here, the amplitude and frequency of the applied field are 2×10^5 V/m and $10\omega_{pe}$, respectively. Blue and red dots correspond to ions and electrons, respectively.	96
5.3	The arrangements of shaped dust particles (dimers), when the number of dimers (a) 19 and (b) 20.	97

A.1 Pictorial representations bound structures of subplots (b), (e), and (g) of Fig. 2.1.	123
--	-----

List of Tables

2.1	Number of polygons in different shells.	41
4.1	Formation of pentagonal structures in radial confinement	83
4.2	Configurations of pentagonal structures formed under different confinement boundaries. Here, the screening parameter $\kappa = 1$	85
4.3	Configurations of pentagonal structures formed under different confinement boundaries when $\kappa=2$	88